


Foliar elemental microprobe data and leaf anatomical traits consistent with drought tolerance in *Eucalyptus largiflorens* (Myrtaceae)

Denise R. Fernando ^{A,C}, Jonathan P. Lynch^B, Meredith T. Hanlon^B and Alan T. Marshall^A

^ADepartment of Ecology, Environment and Evolution, La Trobe University, Bundoora, Vic. 3086, Australia.

^BDepartment of Plant Science, The Pennsylvania State University, University Park, PA 16802, USA.

^CCorresponding author. Email: d.fernando@latrobe.edu.au

Abstract. In food-productive river basins, ecosystems reliant on natural flows are affected by climate change and water removal. One such example is Australia's Murray–Darling Basin (MDB), to which the ecologically important black box tree *Eucalyptus largiflorens* (Myrtaceae) is unique. Little is known about its mineral nutrition and response to flooding. A field study conducted at Hattah Kulkyne National Park on the MDB examined nutrient and Al distribution in mature and young foliage of trees whose status varied with respect to the presence of surface floodwaters. Black box is also of interest due to emerging evidence of its capacity to accumulate high foliar salt concentrations. Here, cryo scanning electron microscopy alone (SEM), combined with energy dispersive spectroscopy (SEM-EDS) and X-ray fluorescence (XRF) spectroscopy were applied to evaluate leaf anatomy and elemental patterns at the cellular and whole-leaf levels. Variation in whole-leaf elemental levels across flooded and dry trees aligned with known nutritional fluctuations in this drought-tolerant species reliant on occasional infrequent flooding. The microprobe data provide evidence of drought tolerance by demonstrating that extended conditions of lack of water to trees do not elicit leaf anatomical changes nor changes to leaf cellular storage of these elements. Foliar Na concentrations of ~2000–6000 mg kg^{−1} DW were found co-localised with Cl in mesophyll and dermal cells of young and mature leaves, suggesting vacuolar salt disposal as a detoxification strategy.

Keywords: *Eucalyptus largiflorens*, black box tree, eucalypt, flooding, watercourses, salinity, Murray–Darling Basin, drought tolerance, foliar microprobe data, riverine ecosystems, river basin system.

Received 22 December 2020, accepted: 3 May 2021, published online 3 June 2021

Introduction

The complexities of managing natural flows within river basin systems to balance their agricultural and native ecological productivities are exacerbated by the rising demand for food and adverse climatic trends (Poff *et al.* 2003; Lynch and St Clair 2004; IPCC 2014; Grafton *et al.* 2018). One such case is the Murray–Darling Basin (MDB), Australia's most agriculturally important and largest river catchment of over 1×10^6 km², also renowned for its significant natural habitats (Pittock and Finlayson 2011). Among many indicators of the health of MDB riverine ecosystems is the condition and persistence of ubiquitous native trees whose crucial ecological services have been documented in some instances as being specific to certain faunal assemblages (O'Malley and Sheldon 1990; NPWS 2002; Wassens *et al.* 2005; Roberts and Marston 2011; Capon *et al.* 2016). Black box (*Eucalyptus largiflorens* Muell. (Myrtaceae)), a floodplain tree largely exclusive to the MDB and belonging to the iconic Australian *Eucalyptus* genus, is one of three common riverine eucalypts in the region (Roberts and Marston 2011;

Capon *et al.* 2016; see also Australia's Virtual Herbarium at <http://avh.chah.org.au>). It is widespread across MDB floodplains, from riparian zones to the farthest reaches of natural flows, and around inland lakes. Although the success of management strategies to sustain riverine woodland ecosystems in the MDB have been mixed, knowledge about their physiology and nutrition is still limited (Bramley *et al.* 2003; Poff *et al.* 2003; Jensen *et al.* 2008; Johns *et al.* 2009; Doody *et al.* 2015; Fernando *et al.* 2018a). As the most notably vulnerable of the MDB riverine eucalypts, the status of black box is of ongoing concern given its poor condition in sections of the MDB (Cunningham *et al.* 2009; Smith and Smith 2014; Moxham *et al.* 2018). Two field studies into its plant–soil nutritional dynamics (Fernando *et al.* 2018a, 2021) provide the only insight into its mineral nutrition, along with emerging evidence of its ability to accumulate high Na concentrations.

Foliar nutrition is synonymous with whole-plant nutrition, a well-established utilitarian measure of the health of terrestrial vascular plants, particularly under cultivation, yet less so for ecological purposes (Grove and Malajczuk 1985; Marschner

2002). In the latter context, macronutrient cycling has drawn significant interest, as has plant adaptation to certain distinct soil types, for example, metallophytes in serpentine ecosystems (Lugo *et al.* 1990; Brooks 1998; Gallardo 2003). The spatial distribution patterns of leaf nutrients and other elements, including cellular sequestrations can indicate certain detoxification strategies, genetic differences, response to altered nutrient supply and environmental change. A range of microprobe techniques utilising X-rays, electron and proton beams are capable of generating plant analytical data *in situ*, both at the intra- and inter-cellular levels, as well as for whole organs such as leaves, depending on size; with electron-beam methodologies further capable of yielding detailed information on tissue anatomy (Fernando *et al.* 2013). There are numerous examples where such techniques applied individually or in combination have contributed valuably to understanding certain plant behaviours. Examples of these include, linking difference in Mn tolerance between two wheat phenotypes to their leaf-vacuolar storage capacity (Fernando *et al.* 2016a), plant salt tolerance through cell storage or specialised glands (Huang and Steveninck 1988; Van Steveninck *et al.* 1988; Oi *et al.* 2013), Mn toxicity observed primarily on the leaf upper surface of field canola due to the interaction of solar radiation with Mn-rich cells (Fernando *et al.* 2016a), and differences in the abilities of two maple species to tolerate soil acidification due to their different leaf anatomies and cellular nutrient storage strategies (Fernando *et al.* 2016b).

Whole-leaf elemental concentrations in inundated black box trees and in those nearby that had remained uninundated for a prolonged period have previously been found to be comparable (Fernando *et al.* 2018a, 2021), consistent with its characterisation as a drought tolerant species (McEvoy 1992). The present investigation seeks to examine whether there are differences in cellular elemental accumulation strategies associated with water availability to trees. Cryo scanning electron microscopy (SEM) and cryo SEM–energy dispersive spectroscopy (SEM-EDS) will be applied to gather leaf anatomical and cellular elemental distributional data, and elemental distributions across entire leaf surfaces will be extracted using XRF. Emerging evidence that black box tolerates high Na concentrations (Fernando *et al.* 2018a) through foliage accumulation will also be investigated by examining Na and Cl localisation in leaf cells.

Materials and methods

Field sampling

The field site, Lake Konardin (34°41'35.05"S, 142°21'2.11"E), is one of numerous interconnecting floodplain lakes in the Hattah Kulkyn National Park, Australia (Fernando *et al.* 2018a). Natural water-flows into these lakes from the Chalka Creek tributary off the Murray River is supplemented by a managed process termed 'environmental watering' where in this case, river water is pumped into the feeder creek (Fernando *et al.* 2021). Three field samplings of black box leaves were conducted as follows, across two time-points linked to a managed watering cycle that was initiated in early July 2017 (a) on 9 December 2017, from an inundated

black box tree that had been receiving floodwaters continuously for at least 3 months before sampling (Fig. 1a); (b) on 9 December 2017, from a black box tree on dry ground, well beyond the reach of floodwaters (Fig. 1b), and (c) on 13 July 2018, from tree (a) at least 5 months after surface waters had fully receded (Fig. 1c). Rainfall data from the Australian Government Bureau of Meteorology website (<http://www.bom.gov.au/>) show that although the site received ~45 mm above its long-term average annual rainfall of 330 mm, there was a total of only ~85 mm in the 7 months between the first and second sampling (Fernando *et al.* 2021). Maximum temperature ranges were ~9°C to 46°C, and minima were ~−1.5 to 30°C. In the field, harvested leaves were stored cool in just-moist packaging so as to retain their field freshness for laboratory processing within 24 h. The youngest fully expanded leaves at the growing tips of branchlets were selected for the 'young' category, and the oldest, highly sclerophyllous, largest leaves lower down along branchlets were selected for the 'mature' category (Fig. 1d). These two categories were visually very distinct. The orientation of mature leaves was vertical as is common among eucalypts (James and Bell 2000), and for the purposes of this study, the outward-most facing surface was designated as the upper surface whereas the other was designated the lower surface.



Fig. 1. Black box sampling (a) flooded tree (arrowed), (b) tree outside flood zone, (c) tree (a) post-flooding, (d) selection of the mature (M) and young (Y) leaves sampled.

Bulk chemical analysis of leaves

The method described by Fernando *et al.* (2018a) was employed here to chemically analyse six leaf samples that each consisted of 10–20 bulked and ground oven-dried material. Total dry weight concentrations (mg kg^{-1}) of the following elements were measured: N, P, K, Ca, Mg, Na, Mn, Al, Fe, and Si. Young and mature leaves were selected as described above for the three samplings. Subsamples of these leaves, while fresh, were prepared for microprobe analysis as described in the following two sections. Bulk leaf-elemental concentration data corresponding to trees selected here for microprobe analyses were obtained to provide context to the microprobe data central to this study. Replicate periodic sampling of these trees had already been undertaken as part of a recent detailed study into leaf and soil elemental changes with respect to flooding (Fernando *et al.* 2021).

Sample preparation for microprobe analyses

Small fragments of excised leaf tissue were rapidly cryo-fixed by plunge freezing in liquid propane, and stored in liquid nitrogen for SEM-EDS as described by Fernando *et al.* (2018b). For X-ray fluorescence spectrometry (XRF), whole fresh leaves were snap-frozen by immersing in liquid nitrogen before being freeze-dried.

SEM, SEM-EDS and XRF analyses

The methodology and instrumentation used for obtaining SEM images and SEM-EDS analytical X-ray map data are detailed in previous studies by Fernando *et al.* (2016a, 2018b). Cryo-fixed frozen leaf samples were planed cross-sectionally on a liquid nitrogen-cooled ultramicrotome (Reichert Jung FC4E, Leica Microsystems), rapidly transferred in a specimen transfer device (Gatan CT1500, Gatan, Pleasanton, CA, USA) to the liquid nitrogen-cooled specimen stage of a scanning electron microscope (SEM) (JEOL JSM 840A, JEOL, Tokyo, Japan) via its liquid nitrogen-cooled preparation chamber (Gatan CT1500). Here, the sample was monitored at 5 kV (to minimise electrical charging) while etched to -90°C , then re-cooled and Al-coated (10 nm) for initial examination on the cold (-180°C) SEM sample stage. For data gathering, the sample was freeze-dried *in situ* and positioned at a stage height of 39 mm, where qualitative and quantitative (Marshall 2017) energy dispersive spectroscopic (EDS) X-ray data as well as secondary electron images (SEI) were collected. An accelerating voltage of 15 kV and a probe current of 2×10^{-10} A was used. These EDS analyses were carried out using an Aztec analyser with an X-Max SDD detector (150 mm^2 , Oxford Instruments, High Wycombe, Buckinghamshire, UK). Qualitative X-ray maps of N, P, K, Mg, Na, and Cl spatial distribution patterns across young and mature leaf cross-sectional surfaces were obtained. Quantitative data for these elements were extracted from the X-ray maps by delineating regions of interest within them as previously undertaken by Fernando *et al.* (2016b). The summed X-ray spectra from these regions were processed using the Oxford Instruments version of the XPP software (see <https://nano.oxinst.com/campaigns/downloads/azteclive-in-depth-tru-q>) according to the methodology of Pouchou

and Pichoir (1991, 1992). These quantitative data are obtained as line-scan traces across a selected tissue area, where the x-axis represents location along tissue, and the y-axis represents:

$$\text{percentage elemental weight} \div \text{tissue dry weight}$$

The latter can be converted to moles per kilogram:

$$\begin{aligned} &(\text{percentage tissue elemental weight} \\ &\div \text{elemental atomic weight}) \times 10 \end{aligned}$$

For XRF, whole leaves or lengthwise halves of cryo-fixed, freeze-dried samples were affixed to a piece of polypropylene sheeting (0.5 mm) with 3M tape (3M Australia, Sydney, NSW, Australia) so that both leaf surfaces were exposed for analysis. Samples were scanned on a Bruker M4 Tornado (Bruker Nano GmbH, Berlin, Germany) equipped with a single rhodium X-ray tube and energy dispersive detector. The maps were created using the Area function over the entire area (mosaic) of each leaf sample placed on a 3-D printed holder covered in cling-wrap so as to retain it 5 cm above the stage surface to minimise background noise from the stage. Scans were performed at a tube voltage of 50 kV and tube wattage of 600 μA under a 20-mbar vacuum with no filter. X-Ray spot size was 20 μm with a pixel size of 100 μm in both x and y directions and a measurement rate of 100 ms pixel $^{-1}$. Semiquantitative data (counts) were extracted from a laminal area of leaves scanned for X-ray maps. Spectra generated within a laminal area were used to calculate net counts by subtracting background counts. For each sample, net counts from the upper and lower leaf-surfaces were averaged to estimate net counts for young and mature leaves from each of the three sampling scenarios (Fig. 1).

Results

Leaf chemical data (Table 1) indicate differences in S, Na, Fe, B, Co, Al, and Si concentrations associated with the flooding status and history of the tree(s) from which respective samples were taken. Note, as indicated in the methodological description, bulk data in Table 1 here provide additional context to the microprobe data, and are consistent with replicate leaf-elemental data obtained in a recent study of this site (Fernando *et al.* 2021). Foliar S concentrations in non-inundated trees (Fig. 1b, c) were higher than in the flooded tree (Fig. 1a), whereas foliar Na concentrations in the flooded tree were found to have almost doubled over the following 7 months when sampled well after waters had subsided, whereas foliage Na in the unflooded tree was comparable to the flooded tree at the time of flooding. The trends in foliage Na concentrations with respect to flooding were also observed for Fe, B, Co, and Al, where the flooding event appeared associated with elevation of these foliar levels at the second sampling. Foliar Si concentrations were much lower in the dry tree that had previously been flooded (Fig. 1c) compared to the tree that remained uninundated throughout the study (Fig. 1b).

Leaf cross sections (Fig. 2) showed that both mature and young leaves of black box are isobilaterally symmetrical, with the mesophyll sandwiched by two epidermal layers within two outermost cuticular layers, the latter present for all mature

Table 1. Analysis of mature and young black box leaves from (a) the flooded tree, (b) a tree that received no floodwaters, (c) tree long after floodwaters had subsided

Leaf sample	N	C	P	K	S	Ca	Mg	Na	Cu	Zn	Mn	Crude protein	Fe	B	Mo	Co	Si	Al	Ni	N:S	N:P	N:K	C:N
	(%)					(mg kg ⁻¹)						(%)				(mg kg ⁻¹)					(units)		
(a) Flooded tree																							
Mature	1.2	51	734	7124	920	11 399	2497	2777	3.0	13	159	7.3	43	58	0.07	0.08	459	17	1.4	13	16	1.6	44
Young	1.6	50	1594	12 015	970	1971	1708	2181	4.7	17	34	9.9	26	11	0.15	0.02	290	9.1	0.80	16	10	1.3	32
(b) Tree that received no floodwaters																							
Mature	0.93	51	1056	4899	1030	15 219	2004	2792	3.7	10	238	5.8	44	85	0.00	0.08	512	20	2.1	9.1	8.8	1.9	55
Young	1.6	50	1861	11 945	1360	3894	1935	3433	8.0	17	60	10.1	39	22	0.14	0.03	546	2.4	2.2	12	8.7	1.4	31
(c) Tree long after floodwaters had subsided																							
Mature	1.1	51	680	7483	1240	10 676	2476	4938	3.4	11	140	7.1	82	86	0.21	0.11	269	48	2.2	9.1	17	1.5	45
Young	1.1	50	623	5735	1190	11 969	2678	5944	3.5	12	167	6.6	111	90	0.16	0.14	290	92	2.8	8.8	17	1.8	47

leaves (Migacz *et al.* 2018). The mesophyll consisted of two 2–3-layer palisade parenchyma cell layers flanking a relatively narrow central spongy parenchyma layer. The distribution patterns of macronutrients in the leaf cross-sectional surfaces (Fig. 2) suggest N distribution across all cell types, whereas P and K were most concentrated in the spongy parenchyma and some palisade parenchyma regions. Foliar Mg was localised in the dermal and mesophyll layers. Cellular Na primarily in the mesophyll with some dermal deposition in young leaves was matched by Cl deposition, although Cl was additionally strongly detected in the spongy mesophyll.

Quantitative SEM-EDS data corresponding to Fig. 2 are represented in Fig. 3, where dry weight tissue concentrations (mmol kg⁻¹) of N, P, K, Mg, Na and Cl can be estimated for different leaf cell types in cross-section. The central linescans of the quantitative X-ray linescan profile data corresponding to each of the six leaf cross sectional surfaces are indicated by red lines in Fig. 2 and yellow lines in Fig. 3.

Whole-leaf XRF elemental maps (Fig. 4) showed that for each element, distribution across two leaf surfaces of a leaf were not different. The Mn map showed a Mn gradient across leaf surfaces such that leaf marginal zones were more Mn-enriched compared to the central laminal area. The microprobe data (Fig. 2–4) all indicate that individual elemental distribution patterns in foliage did not vary qualitatively with the flooding status of the tree.

Net counts in the XRF semiquantitative datasets (Fig. 5) were generally higher for mature leaves compared to young leaves, due in part at least to the greater thickness of the former, with highest observed counts in sampling (b) (Fig. 1b). The thinness of the young leaves likely contributed to the similarity in their upper- and lower-surface XRF semiquantitative data and smaller count numbers. Mature and young leaf laminae from the flooded tree (Fig. 1a) generated the lowest count numbers for all elements examined except P (Fig. 5). Among the three young leaf samples, the post-flooded sample (Fig. 1c) generated highest counts for elements other than P (Fig. 5). Among the three mature-leaf laminae analysed, the non-flooded (Fig. 1b) and post-flooded (Fig. 1c) samples generated far greater count numbers than the flooded sample (Fig. 1a).

Discussion

In-situ microprobe data (Fig. 2, 3) provided the first insights into nutrient and metal distribution patterns in black box leaves

and their anatomy. An isobilateral symmetry, a closely packed mesophyll lacking intercellular spaces, multiple palisade layers, and cuticular coverings were xerophytic features indicative of adaptation to dry conditions (Esau 1965; Migacz *et al.* 2018), as was the vertical positioning of leaves to mitigate water loss and optimise light harvesting while enabling sufficient access to CO₂ for photosynthesis (James and Bell 2000; James and Bell 2001). Except for a single previous study employing XRF to map foliar Pb in a Pb-dosing trial of a *Eucalyptus* hybrid (Rodrigues *et al.* 2018), there is no prior knowledge about elemental micro-distribution patterns in eucalypt leaves. Consistent with existing awareness that black box is drought tolerant (McEvoy 1992) was the overall similarity of individual elemental distribution patterns across the three sample trees (Fig. 2–4); particularly datasets for the wettest (Fig. 1a) and driest (Fig. 1b) growth conditions that showed no clear differences in nutrient sequestration or physical drought-responses such as leaf or cuticular thickening (James and Bell 1995; McLean *et al.* 2014). Highest XRF count rates (Fig. 5) for leaves from the driest tree (Fig. 1b) suggest that they were the thickest in this study.

Bulk leaf-chemical data (Table 1) support recent findings that short-term flooding likely benefits black box by enhancing the soil bioavailability of some trace nutrients, with soil type as an important driver of inundation-associated plant–soil dynamics (White 1997; Fernando *et al.* 2021). Differences observed here in Table 1 are consistent with the findings of a recent detailed study (Fernando *et al.* 2021) of leaf and soil elemental changes with respect to flooding, in which multiple samplings over a 12-month period across an entire flooding cycle demonstrated that inundation was nutritionally advantageous to black box trees. Post-flood lowering of black box leaf Si concentrations has previously been observed (Fernando *et al.* 2021), where concentrations peaked along with flooding and returned to original lower levels after subsidence. Observation of lowest foliage S concentration (Table 1) for the inundated tree (Fig. 1a) aligns with previous findings that foliar S depression is associated with peak inundation, possibly due to biomass dilution by flooding-induced vegetative growth (Fernando *et al.* 2021). Existing hypotheses that drought stress likely depresses leaf-N and -P concentrations by reduced uptake, while increasing N:P concentration ratios (He and Dijkstra 2014) were not supported for black box (Table 1), further consistent with drought tolerance.

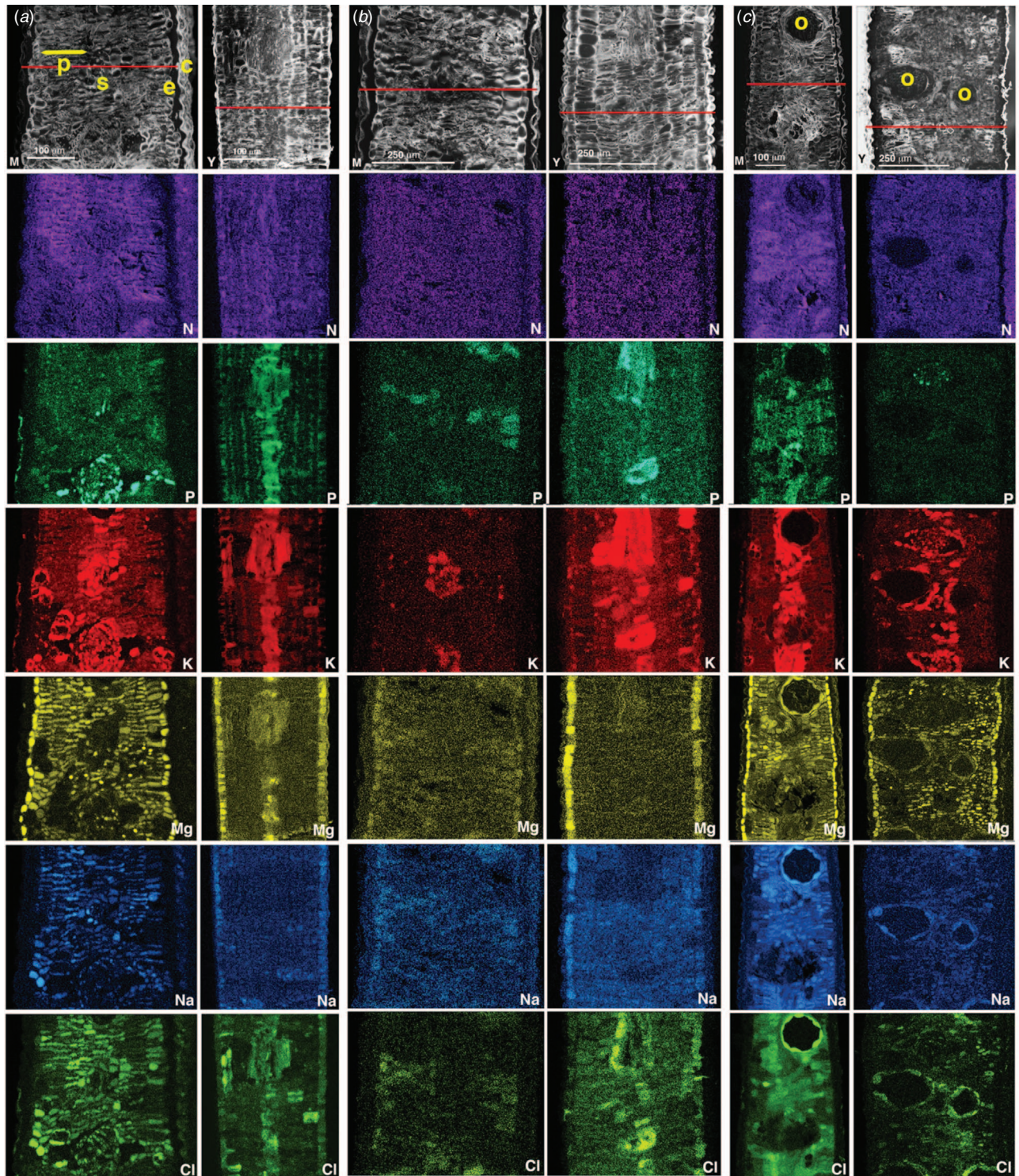


Fig. 2. Cross-sectional SEM anatomical images and corresponding qualitative SEM-EDS X-ray maps showing cellular N, P, K, Mg, Na, and Cl distributions in mature (M) and young (Y) black box leaves from (a) the flooded tree, (b) the tree that did not get flooded, (c) tree (a) well after floodwaters had subsided. Cuticle (c), epidermis (e), spongy parenchyma (s) and palisade parenchyma (p), oil glands (o). Horizontal red lines show central line scan for corresponding quantitative X-ray data shown in Fig. 3.

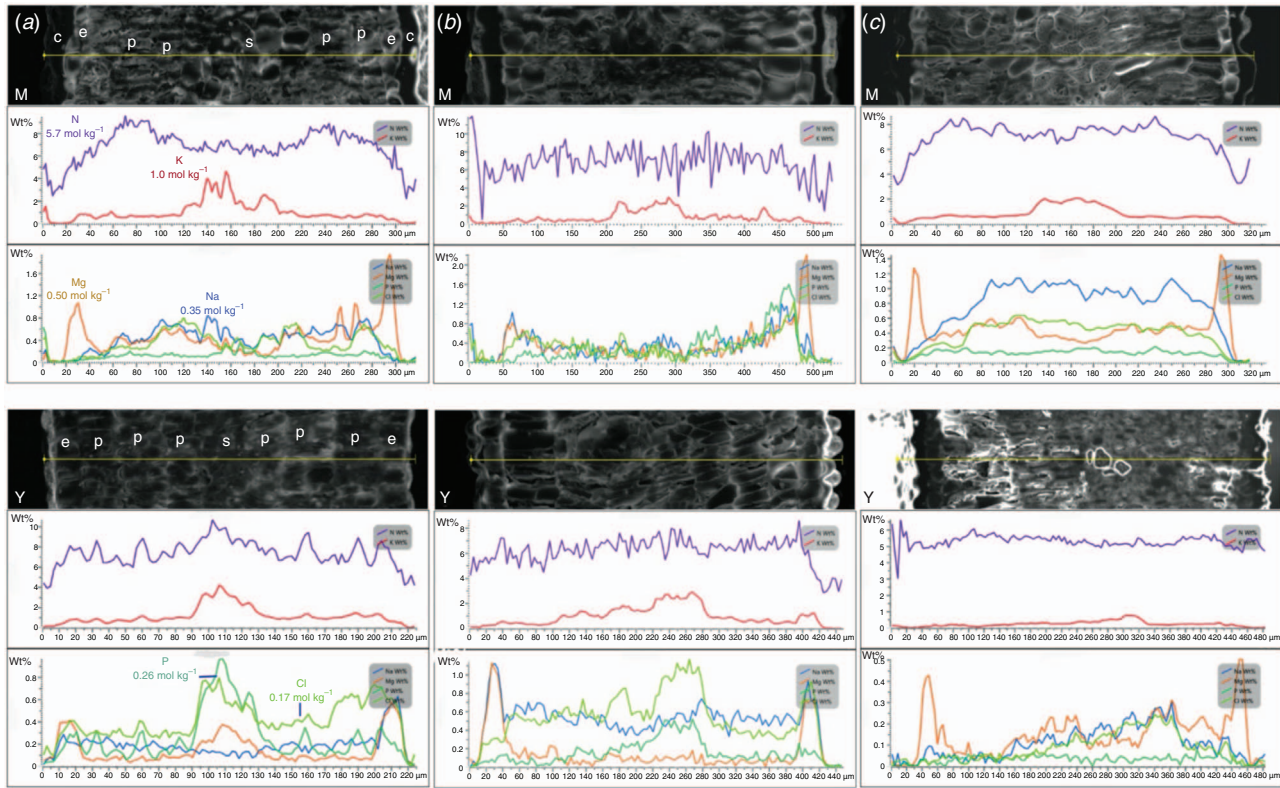


Fig. 3. Quantitative X-ray line-scan profiles (N, K, Na, Mg, P, Cl) collected from entire regions the SEM image above each set of traces, where central scan-lines are marked here in yellow, and appear as red lines in Fig. 2. (a, b, and c) Correspond exactly to those in Fig. 2, for mature (M) and young (Y) black box leaf cross-sectional surfaces. Vertical axis percentage weight elemental concentrations above can be converted to moles per kilogram (dry tissue weight), as shown in (a). Different cell and tissue types labelled (a) are: cuticle (c), epidermis (e), spongy parenchyma (s) and palisade parenchyma (p).

Although there are no previous microprobe studies of eucalypt nutrition to draw upon, cellular N, P, K and Mg accumulation patterns observed here in the cryo SEM-EDS maps (Fig. 2) align with broad understanding around plant nutrition (Judd *et al.* 1996; Marschner 2002; Taiz and Zeiger 2002). The detected presence of N in all cell types and in cuticles (Fig. 2) is likely associated with its ubiquity in proteins, amino acids, enzymes and other major C-compounds (Marschner 2002). The importance of Mg in chlorophyll structure, photosynthesis, enzyme activation, protein synthesis and other functions may explain its detection in all cell types between the cuticular layers as seen in the qualitative X-ray maps (Fig. 2). The photosynthetic capacity of *Eucalyptus* leaves can be maximised as necessary by ground tissue anatomy, depending on climate; for example, with densely packed highly vacuolated palisade cells that are chloroplast-rich and spongy parenchyma cells also containing large numbers of chloroplasts (Evans and Vogelmann 2006; Eltahir *et al.* 2018). Greater P and K localization in the vasculature and spongy cells compared to surrounding palisade cells (Fig. 2) may be due to the high mobility of orthophosphate and K ions (Taiz and Zeiger 2002). Spongy cells usually have larger cytoplasmic-to-vacuolar volume ratios, unlike palisade cells where the converse applies (Esau 1965); with cytoplasmic K concentrations

generally exceeding those of vacuoles in higher plants at least (Leigh and Jones 1984). The quantitative X-ray line-scan data (Fig. 3) extracted from the qualitative maps (Fig. 2) support the latter. Highest K levels are in the central spongy parenchyma, whereas Na is consistently observed in mesophyll cells. Some epidermal Na storage was found in young leaves of treatments (a) and (b), whose Cl storage was highest in the spongy parenchyma and palisade. Magnesium was mostly highly localised in the epidermal cell layers.

Elevated foliar Na concentrations of ~2000–6000 mg kg⁻¹ observed here (Table 1) add to emerging evidence that black box at the Hattah Lakes site is highly salt tolerant by foliage accumulation (Fernando *et al.* 2018a, 2021); warranting wider geographic investigation of this species. Previously published foliar-Na concentrations for mature riverine eucalypts are typically ~2500 mg kg⁻¹, with values ~1900 and 6500 mg kg⁻¹ reported respectively for *E. camaldulensis* and *E. largiflorens* (Judd *et al.* 1996; Hulme and Hill 2005; Fernando *et al.* 2021). ‘Normal’ plant requirement for the essential micronutrients Na and Cl are ~10 and 300 mg kg⁻¹ respectively in foliage, although Cl is widely known to accumulate to much higher concentrations (Taiz and Zeiger 2002). The main nutritional roles of Na are as a metabolite shuttle in C4 grasses and halophytes, and infrequent substitution for K, whereas Cl serves as a highly mobile

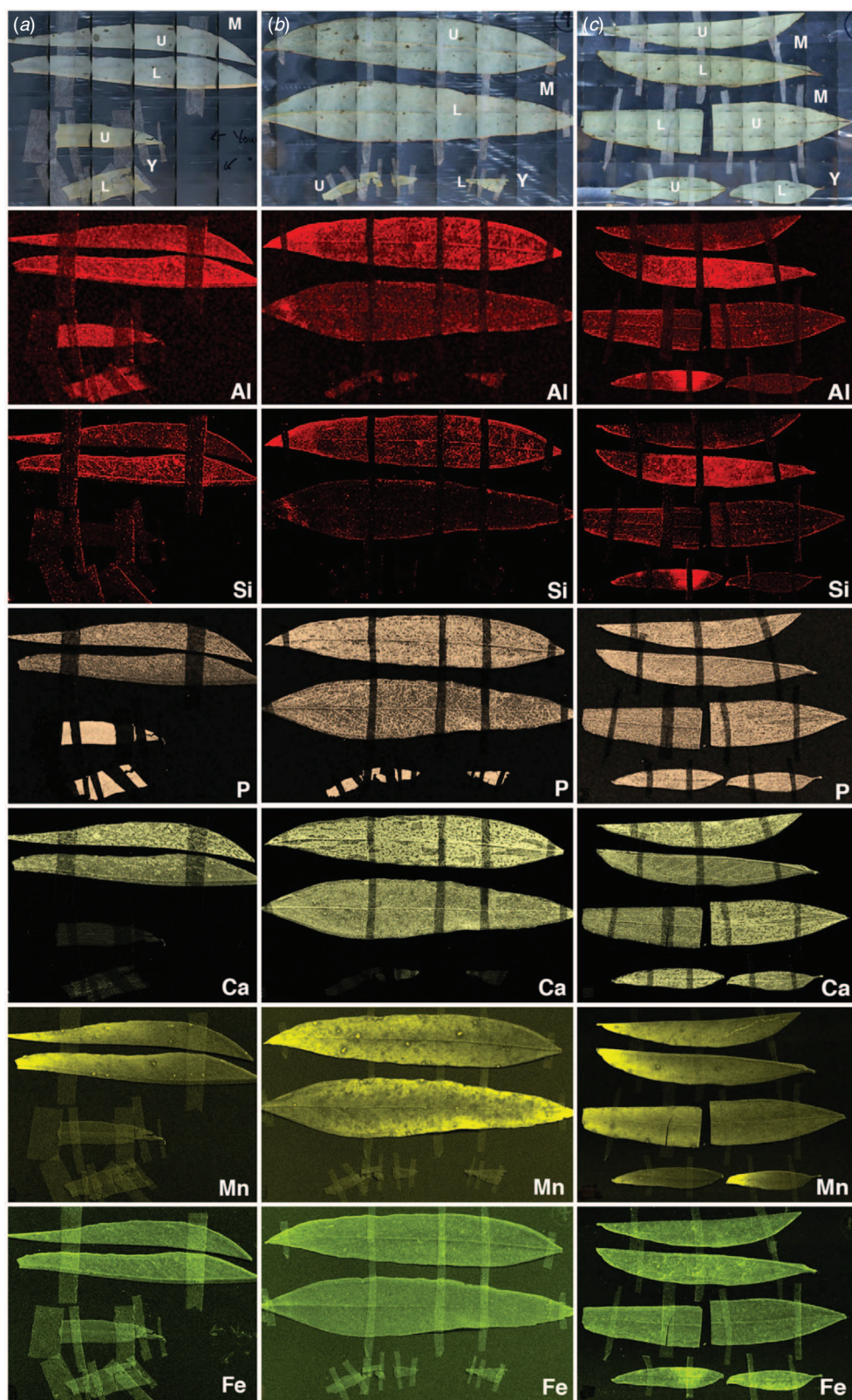


Fig. 4. Sample photographs and corresponding XRF maps of Al, Si, P, Ca, Mn, and Fe distributions in mature (M) and young (Y) leaves from (a) the flooded tree, (b) a tree that received no floodwaters, (c) tree (a) long after floodwaters had subsided. Upper (U) and lower (L) leaf surfaces shown.

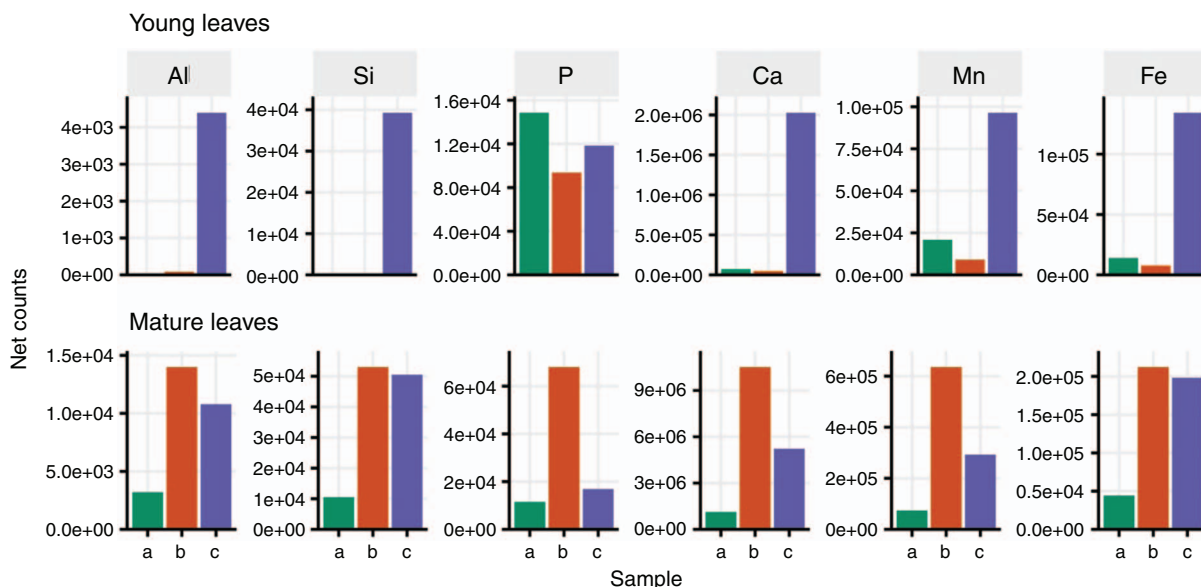


Fig. 5. Semiquantitative XRF data for Al, Si, P, Ca, Mn, and Fe in young and mature leaves from (a) the flooded tree, (b) a tree that received no floodwaters, (c) tree (a) long after floodwaters had subsided.

inorganic anion involved in charge compensation and osmoregulation (Taiz and Zeiger 2002). Detection here of Cl and not Na in the central spongy area and vascular tissue may be due to this high mobility and essential role. Bulk leaf Na concentrations can be interpreted as a proxy for salt accumulation capacity (Acosta-Motos *et al.* 2017), but the detection of Cl in cells containing Na (Fig. 2) suggests co-localisation. Since it is well established that vacuolar sequestration is a common plant detoxification strategy (Fernando *et al.* 2013; Munns and Gilliham 2015), it is plausible that excess NaCl in black box foliage is stored in vacuolar compartments. Furthermore, salt stress studies of other Myrtaceae species have linked the expansion of leaf intercellular spaces to salt stress (Acosta-Motos *et al.* 2017), which was not evident in the SEM leaf anatomical images (Fig. 2).

Whole-leaf elemental XRF maps of mature and young leaf surfaces (Fig. 4) were consistent with their vertical positioning and isobilateral symmetry given that for each sample, leaf-surface distributions of individual elements did not vary markedly between upper and lower surfaces, with the exception of some inter-surface differences in young leaves. There is limited scope for interpreting XRF maps (Fig. 4) against bulk leaf data (Table 1) since XRF data comprise signals from varying sample depths, with signal strength determined by sample thickness, matrix and the element of interest (Rodrigues *et al.* 2018). According to these authors who trialled an *Eucalyptus* leaf, samples used in this present study may be regarded as sufficiently 'thin' to generate XRF maps (Fig. 4) representing the entire leaf thickness. Comparison of young leaf data within each of the two XRF datasets in this study (Fig. 4, 5) suggest an increase in foliar elements associated with flooding; with enhanced Al, Si, Ca, Mn, and Fe accumulation on at least one surface (Fig. 4). As in

the cryo SEM-EDS maps (Fig. 2), the similarity of leaf-surface XRF distribution patterns for each individual element across the three different flooding states indicates drought resistance. The distinct gradient in Mn distribution across the leaf surface (Fig. 4) from lowest to highest approaching leaf marginal areas has previously been explained as being due to higher transpiration rates at the leaf margins (Millikan 1951; Blamey *et al.* 2015; Fernando *et al.* 2016a).

In demonstrating elemental distribution patterns in black box leaves with reference to anatomy, these findings highlight aspects of the ability of this species to tolerate dry conditions. The study also provides new insight into the capacity of black box at Hattah to accumulate high foliar salt concentrations, which warrants a species-wide examination of the trait across its wider geographic distribution. The use of analytical microprobe methodologies to interrogate leaf mineral nutrient distribution patterns was applied for the first time to a *Eucalyptus* species, where the role of some macronutrients at least as interpreted from data obtained here, align with existing knowledge of their plant functions, and more recent understanding of the nutritional benefits of flooding.

Conflicts of interest

The authors declare that they have no conflicts of interest.

Declaration of funding

This research was funded by Eucalypt Australia and the Australian Research Council (grant number 120100510).

Acknowledgements

We thank Parks Victoria for supporting our field collections.

References

- Acosta-Motos JR, Ortuno MF, Bernal-Vicente A, Diaz-Vivancos P, Sanchez-Blanco MJ, Hernandez JA (2017) Plant responses to salt stress: adaptive mechanisms. *Agronomy* **7**(1), 18. doi:10.3390/agronomy7010018
- Blamey FP, Hernandez-Soriano MC, Cheng M, Tang C, Paterson DJ, Lombi E, Wang WH, Scheckel KG, Kopittke PM (2015) Synchrotron-based techniques shed light on mechanisms of plant sensitivity and tolerance to high manganese in the root environment. *Plant Physiology* **169**, 2006–2020. doi:10.1104/pp.15.00726
- Bramley H, Hutson J, Tyerman SD (2003) Floodwater infiltration through root channels on a sodic clay floodplain and the influence on a local tree species *Eucalyptus largiflorens*. *Plant and Soil* **253**, 275–286. doi:10.1023/A:1024531325281
- Brooks RR (1998) 'Plants that Hyperaccumulate Heavy Metals.' (CAB International: Oxon, UK)
- Capon S, James CS, George AK (2016) Riverine trees and shrubs. In 'Vegetation of Australian Riverine Landscapes: Biology, Ecology and Management'. (Eds CJS Capon, M Reid) pp. 119–142. (CSIRO Publishing: Melbourne, Vic., Australia)
- Cunningham S, MacNally R, Griffioen P, White M (2009) Mapping the condition of river red gum and black box stands in The Living Murray icon sites. MDBA. Report book number 51/10, Murray–Darling Basin Authority, Canberra, ACT, Australia.
- Doody TM, Colloff MJ, Davies M, Koul V, Benyon RG, Nagler PL (2015) Quantifying water requirements of riparian river red gum (*Eucalyptus camaldulensis*) in the Murray–Darling Basin, Australia – implications for the management of environmental flows. *Ecohydrology* **8**, 1471–1487. doi:10.1002/eco.1598
- Eltahir AS, Elkamali HH, Abdallah SA, Hamad SF (2018) Comparative study of anatomy of *Eucalyptus Microtheca* and *Eucalyptus camaldulensis* leaves. *Journal of Faculty of Sciences* **5**, 84–94.
- Esau K (1965) 'Plant Anatomy.' (Wiley: New York, NY, USA)
- Evans JR, Vogelmann TC (2006) Photosynthesis within isobilateral *Eucalyptus pauciflora* leaves. *New Phytologist* **171**, 771–782. doi:10.1111/j.1469-8137.2006.01789.x
- Fernando DR, Marshall A, Baker AJM, Mizuno T (2013) Microbeam methodologies as powerful tools in manganese hyperaccumulation research: present status and future directions. *Frontiers in Plant Science* **4**, 319. doi:10.3389/fpls.2013.00319
- Fernando DR, Moroni SJ, Scott BJ, Conyers MK, Lynch JP, Marshall AT (2016a) Temperature and light drive manganese accumulation and stress in crops across three major plant families. *Environmental and Experimental Botany* **132**, 66–79. doi:10.1016/j.envexpbot.2016.08.008
- Fernando DR, Marshall AT, Lynch JP (2016b) Foliar nutrient distribution patterns in sympatric maple species reflect contrasting sensitivity to excess manganese. *PLoS One* **11**, e0157702. doi:10.1371/journal.pone.0157702
- Fernando DR, Lynch JP, Reichman S, Clark G, Miller R, Doody T (2018a) Inundation of a floodplain lake woodlands system: nutritional profiling and benefit to mature *Eucalyptus largiflorens* (Black Box) trees. *Wetlands Ecology and Management* **26**, 961–975. doi:10.1007/s11273-018-9623-x
- Fernando DR, Marshall AT, Green PT (2018b) Cellular ion interactions in two endemic tropical rainforest species of a novel metallophytic tree genus. *Tree Physiology* **38**, 119–128. doi:10.1093/treephys/tpx099
- Fernando DR, Fernando AE, Koerber GR, Doody TM (2021) Tree-soil interactions through water release to a floodplain ecosystem: a case study of Black Box (*Eucalyptus largiflorens*) on loamy sands. *Wetlands* doi:10.1007/s13157-021-01419-4
- Gallardo A (2003) Effect of tree canopy on the spatial distribution of soil nutrients in a Mediterranean Dehesa. *Pedobiologia* **47**, 117–125. doi:10.1078/0031-4056-00175
- Grafton RQ, Williams J, Perry CJ, Molle F, Ringler C, Steduto P, Udall B, Wheeler SA, Wang Y, Garrick D, Allen RG (2018) The paradox of irrigation efficiency: higher efficiency rarely reduces water consumption. *Science* **361**, 748–750. doi:10.1126/science.aat9314
- Grove TS, Malajczuk N (1985) Nutrient accumulation by trees and understorey shrubs in an age-series of *Eucalyptus diversicolor* F.Muell. stands. *Forest Ecology and Management* **11**, 75–95. doi:10.1016/0378-1127(85)90059-3
- He M, Dijkstra FA (2014) Drought effect on plant nitrogen and phosphorus: a meta analysis. *New Phytologist* **204**, 924–931. doi:10.1111/nph.12952
- Huang CX, Steveninck RFMV (1988) Effect of moderate salinity on patterns of potassium, sodium and chloride accumulation in cells near the root tip of barley: Role of differentiating metaxylem vessels. *Physiologia Plantarum* **73**, 525–533. doi:10.1111/j.1399-3054.1988.tb05436.x
- Hulme K, Hill S (2005) Mineralisation discovery through transported cover using River Redgums (*Eucalyptus camaldulensis*). In 'Minerals Exploration Seminar', 25 May 2005, Perth, WA, Australia. (Ed. RAD Gee) pp. 31–33. (CRC LEME: Perth, WA, Australia) Available at http://crlcme.org.au/NewsEvents/Events/Minex%20Seminar%20May%2005/Abstract_Volume_Minex%20May05.pdf
- IPCC (2014) 'IPCC, 2014: Summary for Policymakers.' (Cambridge University Press: Cambridge, UK, and New York, NY, USA)
- James SA, Bell DT (1995) Morphology and anatomy of leaves of *Eucalyptus camaldulensis* clones: variation between geographically separated locations. *Australian Journal of Botany* **43**, 415–433. doi:10.1071/BT9950415
- James SA, Bell DT (2000) Leaf orientation, light interception and stomatal conductance of *Eucalyptus globulus* ssp. *globulus* leaves. *Tree Physiology* **20**, 815–823. doi:10.1093/treephys/20.12.815
- James SA, Bell DT (2001) Leaf morphological and anatomical characteristics of heteroblastic *Eucalyptus globulus* ssp. *globulus* (Myrtaceae). *Australian Journal of Botany* **49**, 259–269. doi:10.1071/BT99044
- Jensen AE, Walker KF, Paton DC (2008) The role of seedbanks in restoration of floodplain woodlands. *River Research and Applications* **24**, 632–649. doi:10.1002/tra.1161
- Johns C, Reid CJ, Roberts J, Sims N, Doody T, Overton I, McGinness HM, Rogers K, Campbell C, Gawne B (2009) Native trees of the River Murray floodplain: literature review and experimental designs to examine effects of flow enhancement and floodwater retention. Final report for the MDBA, Murray–Darling Freshwater Research Centre, Wodonga, Vic., Australia.
- Judd TS, Attiwill PM, Adams MA (1996) Nutrient concentrations in *Eucalyptus*: a synthesis in relation to differences between taxa, sites and components. In 'Nutrition of Eucalypts'. (Eds PM Attiwill, MA Adams) pp. 123–153. (CSIRO Publishing: Melbourne, Vic., Australia)
- Leigh RA, Jones RG (1984) A hypothesis relating critical potassium concentrations for growth to the distribution and functions of this ion in the plant cell. *New Phytologist* **97**, 1–13. doi:10.1111/j.1469-8137.1984.tb04103.x
- Lugo AE, Cuevas E, Sanchez MJ (1990) Nutrients and mass in litter and top soil of ten tropical tree plantations. *Plant and Soil* **125**, 263–280. doi:10.1007/BF00010665
- Lynch JP, St Clair SB (2004) Mineral stress: the missing link in understanding how global climate change will affect plants in real world soils. *Field Crops Research* **90**, 101–115. doi:10.1016/j.fcr.2004.07.008
- Marschner H (2002) 'Mineral Nutrition of Higher Plants.' (Academic Press: London, UK)
- Marshall AT (2017) Quantitative X-ray microanalysis of model biological samples in the SEM using remote standards and the XPP analytical model. *Journal of Microscopy* **266**, 231–238. doi:10.1111/jmi.12531

- McEvoy PK (1992) Ecophysiological comparisons between *Eucalyptus camaldulensis* Denh., *E. largiflorens* F.Muell. and *E. microcarpa* (Maiden) Maiden on the River Murray Floodplain. University of Melbourne, Melbourne, Vic., Australia.
- McLean EH, Prober SM, Stock WD, Steane DA, Potts BW, Vaillancourt RE, Byrne M (2014) Plasticity of functional traits varies clinally along a rainfall gradient in *Eucalyptus tricarpa*. *Plant, Cell & Environment* **37**, 1440–1451. doi:10.1111/pce.12251
- Migacz IP, Raeski PA, Almeida VP, Raman V, Nisgoski S, Muniz GI, Farago PV, Khan IA, Budel JM (2018) Comparative leaf morpho-anatomy of six species of *Eucalyptus* cultivated in Brazil. *Brazilian Journal of Pharmacognosy* **28**, 273–281. doi:10.1016/j.bjp.2018.04.006
- Millikan CR (1951) Radio-autographs of manganese in plants. *Australian Journal of Biological Sciences* **4**, 28–41. doi:10.1071/B19510028
- Moxham C, Duncan M, Moloney P (2018) Tree health and regeneration response of Black Box (*Eucalyptus largiflorens*) to recent flooding. *Ecological Management & Restoration* **19**, 58–65. doi:10.1111/emr.12288
- Munns R, Gilliam M (2015) Salinity tolerance of crops – what is the cost? *New Phytologist* **208**, 668–673. doi:10.1111/nph.13519
- NPWS (2002) Biodiversity survey. Technical report, Dubbo, NSW, Australia.
- O'Malley C, Sheldon F (1990) 'Chowilla Floodplain Biological Study.' (Nature Conservation Society of South Australia: Adelaide, SA, Australia)
- Oi T, Hirunagi K, Taniguchi M, Miyake H (2013) Salt excretion from the salt glands in Rhodes grass (*Chloris gayana* Kunth) as evidenced by low-vacuum scanning electron microscopy. *Flora* **208**, 52–57. doi:10.1016/j.flora.2012.12.006
- Pittock J, Finlayson CM (2011) Australia's Murray–Darling Basin: freshwater ecosystem conservation options in an era of climate change. *Marine and Freshwater Research* **62**, 232–243. doi:10.1071/MF09319
- Poff NL, Allen JD, Palmer MA, Hart DD, Richter BD, Arthington AH, Rogers KH, Meyer JL, Stanford JA (2003) River flows and water wars: emerging science for environmental decision making. *Frontiers in Ecology and the Environment* **1**, 298–306. doi:10.1890/1540-9295(2003)001[0298:RFAWWE]2.0.CO;2
- Pouchou JL, Pichoir F (1991) Quantitative analysis of homogeneous or stratified microvolumes applying the model 'PAP'. In 'Electron Probe Quantitation'. (Eds KFJ Heinrich, DE Newbury) pp. 31–75. (Plenum Press: New York, NY, USA)
- Pouchou JL, Pichoir F (1992) Advanced quantitative procedures for analytical SEM and EPMA: X-ray microanalysis of light elements and layered specimens. In 'Electron Microscopy, EUREM 92', 7–11 September 1992, Granada, Spain. Vol. 1, pp. 293–297. (European Congress on Electron Microscopy: Granada, Spain)
- Roberts J, Marston F (2011) 'Water Regime of Wetland & Floodplain Plants in the Murray–Darling Basin.' (National Water Commission: Canberra, ACT, Australia)
- Rodrigues ES, Gomes MHF, Duran NM, Cassanji JGB, daCruz TNM, Neto ASA, Savassa SM, DeAlmeida E, Carvalho HWP (2018) Laboratory microprobe X-ray fluorescence in plant science: emerging applications and case studies. *Frontiers in Plant Science* **9**, 1588. doi:10.3389/fpls.2018.01588
- Smith P, Smith J (2014) Floodplain vegetation of the River Murray in 1987–1988: an important pre-drought benchmark for subsequent studies. *Cunninghamia* **14**, 97–151. doi:10.7751/cunninghamia.2014.14.007
- Taiz L, Zeiger E (2002) 'Plant Physiology', 3rd edn. (Sinauer Associates Inc.: Sunderland, MA, USA)
- Van Steveninck RFM, Fernando DR, Anderson CA, Edwards LB, Van Steveninck ME (1988) Chloride and sulphur concentrations in chloroplasts of spinach. *Physiologia Plantarum* **74**, 651–658. doi:10.1111/j.1399-3054.1988.tb02031.x
- Wassens S, Car C, Jansen A (2005) 'Murrumbidgee Irrigation Area Invertebrate Biodiversity Benchmark.' (Murrumbidgee Irrigation Ltd: Griffith, NSW, Australia)
- White RE (1997) 'Principles and Practices of Soil Science – the Soil as a Natural Resource.' (Blackwell Science: Melbourne, Vic., Australia)

Handling editor: Lynda Prior